INTEGRATED LAB JOURNAL ISSN 2339-0905
DOI : 10.5281/zenodo.1904920

CHARACTERISTICS OF BOILING BUBBLE DEPARTURE DIAMETER AND FREQUENCY FROM POROUS FOAM STRUCTURES

Indro Pranoto[1*], Umar Fadhil Ramadhan[1], Muhammad Habtry[1] and Leong Kai Choong[2]

[1]Department of Mechanical and Industrial Engineering, Faculty of Engineering, Universitas Gadjah Mada, Jl. Grafika No. 2 Kampus UGM, Yogyakarta, 55281, Indonesia

[2]School of Mechanical and Aerospace Engineering, Nanyang Technological University, 50 Nanyang Avenue, 639798, Singapore

*E-mail: indro.pranoto@ugm.ac.id

Abstract

An experimental study on the boiling phenomena and bubble dynamics from the porous graphite foams of different thermophysical properties with FC-72 dielectric coolant under saturated pool boiling condition is presented in this paper. The pool boiling process from different graphite foams viz. "Pocofoam" of 61%, "Pocofoam" of 75%, "Kfoam" of 78% and "Kfoam" of 72% porosities were captured by using a high speed camera at 2005 frames per second and analyzed by using "Image Pro" image processing software. The bubble departure diameter and frequency from the porous foams are presented and discussed in this study. The results show that "Pocofoam" of 61% porosity has produced the smallest bubble departure diameter and highest bubble departure frequency as compared to other porous foams. It was found that the average bubble departure diameter and bubble frequency of "Pocofoam" of 61% porosity is 480.8 μm and 173 Hz, respectively. The experimental results have also shown that the thermal properties of the porous graphite foam affected the bubble departure diameter and frequency.

Keywords: *Pool Boiling, Porous Foam, Bubble Dynamics, Departure Frequency, Bubble Diameter, Two-Phase Cooling*

INTRODUCTION

Current and future industrial development which is required an advanced electronic devices and internet of things system drive a constant need on the design of new generation of electronics devices with very high power densities and performance. The decrease of size versus increase of processor speed has caused the decrease of heat transfer surface area which leads to very high heat fluxes. The power density level of high performance electronic devices is projected to reach 200 W/cm^2 in the years 2014 – 2020 (ITRS, 2007). As elaborated by Mudawar (2001), cooling technologies for electronic devices have shifted from natural convection to single-phase forced convection and then to phase-change cooling systems. The heat transfer performance limitations of natural and single phase forced convection have driven the development of two-phase cooling or boiling heat transfer. Hence, two-phase cooling is generally considered to be one of the promising techniques for high heat flux electronic devices in the future. The bubble departure diameter (D_B) and frequency (f_B) are important parameters in bubble dynamics that directly affect boiling heat transfer performance. Surface heating, liquid heating, nucleation, bubble growth and departure occur continuously and repeatedly during the boiling process such that the cycle is normally known as an ebullition cycle.

During the boiling process, a bubble is generated from an activated cavity on the boiling surface. The generated bubble grows during the bubble growth time and then departs from the nucleation cavity. The bubble diameter at the time of departure from the nucleation site is called the bubble departure diameter. The bubble departure frequency indicates how fast the bubble grows and departs from the cavity. It is affected directly by the bubble departure

diameter. At the same heat flux, a smaller bubble departure diameter will result in a higher bubble departure frequency.

During the previous decade, studies on the bubble departure diameter and frequency measurement and predictions were conducted by many researchers. The bubble growth mechanism and parameters from the smooth boiling surfaces have been studied experimentally and analytically by Forster and Zuber (1955), Han and Griffith (1965), and Cole and Rohsenow (1968). Bubble dynamics from artificial structured surfaces were experimentally and analytically studied by Nakayama *et al*. (1980). Bubble departure diameter and frequency predictions were proposed from their works. In their model, bubble dynamics from the structured surface are categorized into three phases: pressure build-up, pressure reduction and liquid intake. Their D_B model is expressed as

$$D_B = C_B \left[\frac{2\sigma}{g\left(\rho_l - \rho_v\right)} \right]^{1/2} \tag{1}$$

Haider (1994) proposed the following equation for constant C_B:

$$C_B = \left(3 s_g \sin\theta\right) \left[\frac{2\sigma}{g\left(\rho_l - \rho_v\right)} \right]^{-1/6} \tag{2}$$

where s_g is the surface gap width of the boiling system.

Chien and Webb (1998) conducted a visualization and analytical study on the bubble dynamics from the structured surface with a circular fin base. Their structure surface possessed surface pores and sub-surface tunnels to enhance the boiling surface area and the bubble escaping process. Semi-analytical models of the bubble departure diameter and frequency were proposed from their study. They stated that their models could predict the bubble departure diameter and bubble frequency with accuracies of ±20% and ±30%, respectively to their experimental data. Their D_B and f_B models are expressed as

$$D_B = \left[\frac{Bo + \sqrt{Bo^2 + 2304(96/Bo - 3)}}{192 - 6Bo} \right]^{1/2} d_P \tag{3}$$

$$f_B = \frac{1}{0.0296 \left[\frac{7}{\pi} \frac{\rho_l T_W}{h_{lv} \rho_v \Delta T_{sat}} \frac{\left(D_B + d_P\right)}{\left(D_B - d_P\right)} \right]^{1/2} \left(\frac{D_B - d_P}{2} \right)} \tag{4}$$

Dhir *et al*. (2007) studied the bubble departure and frequency by simulations and experiments of pool and flow boiling. The simulations were based on the solution of the conservation equations of mass, momentum, and energy for both phases. In their study, the interface shape was captured through a level set function. Comparisons of the bubble shape during evolution, bubble diameter at departure, and bubble growth period were made with data from their experiments. Furberg (2011) conducted bubble dynamics investigation and proposed a model for f_B and D_B on a dendiritic and micro-porous structure. The bubble frequency was determined based on the heat and mass balance during the nucleation process

while the bubble diameter was determined by balancing the forces acting on the micro-structure surface. The bubble frequency is expressed as

$$\frac{f_B}{P} = \frac{q''_{lat} / P}{V_B \Delta h_{lv} \rho_v} \tag{5}$$

From the above brief literature survey, it can be concluded that there are limited studies on bubble dynamics from porous structures in general and porous foam structures in particular. This study focuses on the experimental study to determine the bubble departure diameter and frequency from porous graphite foam structures with dielectric coolants. The results of this study would yield better understanding of the bubble dynamics from the porous graphite foam structures that have been proven to enhance boiling heat performance and are becoming a promising material for cooling electronic components in the near future [Klett and Trammel (2004); White *et al*. (2005); Williams and Roux (2006); Jin *et al*. (2011); Pranoto *et al*. (2012)].

EXPERIMENTAL DESIGN

Experimental Facility. A compact pool boiling experimental setup was developed to study the bubble departure diameter and frequency from the porous graphite foams. The facility consists of three main parts: heating base, evaporator, and air-cooled condenser as shown in Figure 1. A customized cartridge heater is inserted at the centre of a Teflon heating base to generate heat. The ceramic insulation layer and Teflon base effectively minimised the heat loss during the experiments. To adjust the level of generated heat, a power controller was used. The maximum heat flux achievable is 1.5×10^3 kW/m^2. A "Carlo Gavazzi WM14-96" power meter was used to monitor the level of generated heat. The graphite foam evaporator insert was bonded on a copper plate by using highly thermal conductive epoxy "OMEGABOND 101". The designed copper plate was clamped tightly on the heater surface and properly sealed with the adhesive. The heater was fastened to provide good contact at the interface between the top of the heater and the copper plate. A rubber O-ring was employed at the interface between the copper plate and Teflon surface to improve liquid tightness.

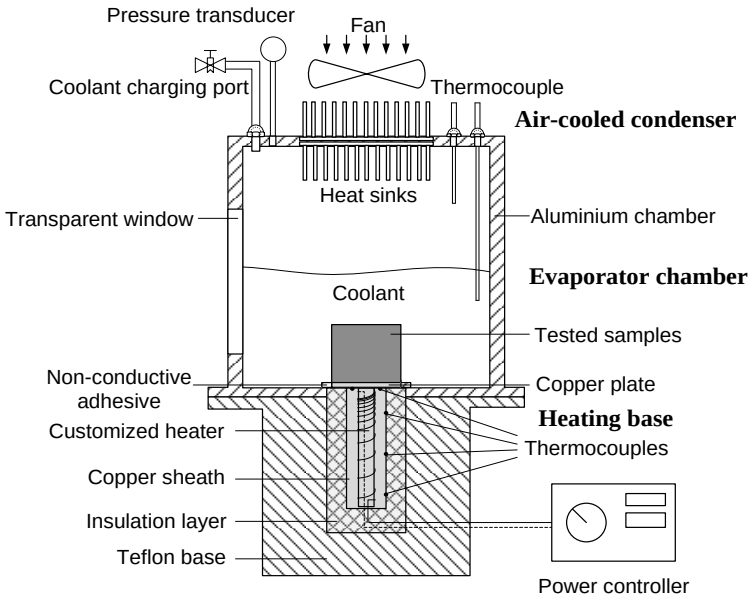

Figure 1. Schematic Diagram of the Pool Boiling Facility.

Seven (7) type K thermocouples were used to measure the temperatures of the liquid, vapor, wall and locations along the heater. The wall temperature was determined from the average temperature measured by two thermocouples attached on the copper plate surface.

The rectangular evaporator chamber is made of aluminum with a transparent polycarbonate window installed on a side wall to allow the boiling process to be observed. The chamber was clamped tightly on the heating base by flange connection and sealed with rubber O-rings to secure the air and liquid leakages. The chamber was filled with the coolant through a charging port. The pressure inside the chamber was measured by an "OMEGA PX409" pressure transducer. On the top section, an air-cooled condenser was installed on the aluminum cover with a thermally conductive paste "OMEGATHERM 201" filling the interface. The top cover was clamped tightly to the chamber and sealed with a rubber O-ring. The condenser consists of two copper pin fin arrays attached on two sides of the top cover. The condensed vapor returns to the evaporator section by gravity. To enhance the heat removal from the condenser, a 300-mm diameter AC fan ("ORIX 18W") was installed. To study the bubble departure diameter and departure frequency, a "Fastec Hispec" high speed camera at 2005 frames per second were used to capture the boiling process. The captured boiling images were processed and analyzed by using "Image Pro" software to determine the bubble departure diameter and frequency.

Porous Graphite Foams. In this study, four types of graphite foam with different thermophysical properties *viz*. "Pocofoam" of 61% porosity, "Pocofoam" of 75% porosity, "Kfoam" of 78% porosity, and "Kfoam" of 72% porosity were applied as an evaporator insert. The internal structures of the graphite foams obtained by Scanning Electron Microscope (SEM) are shown in Figure 2. All samples were fabricated into cubes of dimensions 30(*L*) × 30(*W*) × 20(*H*) (mm) by Wire Cut Electron Discharge Machining (EDM). The pertinent properties of the graphite foam provided by the manufacturer are presented in Table 1.

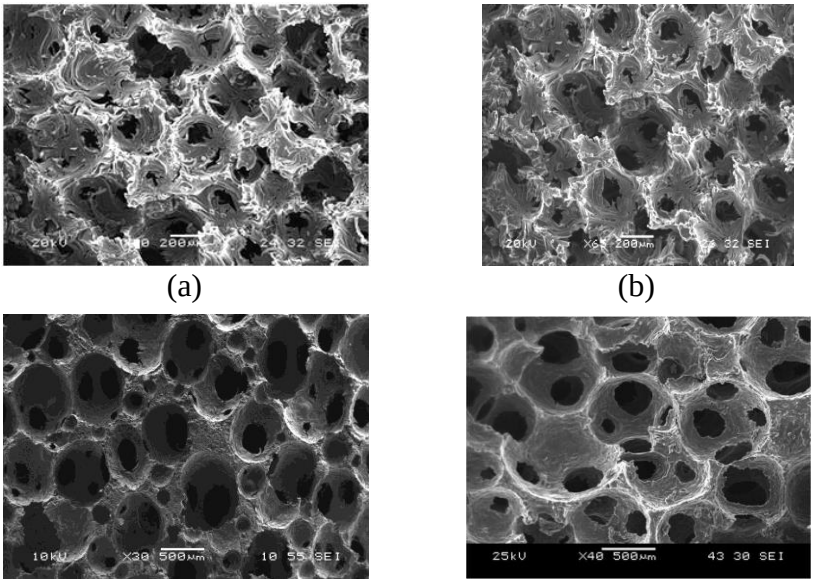

Figure 2. SEM Images of Graphite Foams (a) "Pocofoam" 61%, (b) "Pocofoam" 75%, (c) "Kfoam" 78% and (d) "Kfoam" 72%.

Table 1. Pertinent Properties of the Foams [Poco (2011), Koppers (2011)].

Properties	"Pocofoam" 61%	"Pocofoam" 75%	"Kfoam" 72%	"Kfoam" 78%
d_p (μm)	350	350	650	500
ε (%)	61	75	72	78
ρ (g/cm³)	0.90	0.50	0.48	0.34
k_{eff} (W/m·K)	245	135	110	55

Working Fluids. In this study, FC-72 dielectric liquid from 3M Ltd., USA was chosen as working fluid. This phase change liquid is commonly used for cooling electronic devices or in other thermal management schemes. Both these fluids are thermally and chemically stable, non-flammable, and practically non-toxic and have low Global Warming Potential (GWP). The selected thermal and physical properties at of the coolants at 25ºC and 1 atm are shown in Table 2.

Table 2. Physical and Thermal Properties of FC-72 (3M, 2009)

Properties	Values
Boiling point [ºC]	56
Vapour pressure [kPa]	30.9
Liquid density [kg/m³]	1680
Specific heat [J/(kg·°C)]	1100
Latent heat of vaporization [kJ/kg]	88
Thermal conductivity [W/m□K)]	0.057
Surface tension [mN/m]	10
Dielectric strength [kV]	38

Data Reduction and Uncertainty Analysis. All temperature and pressure signals are acquired by a "YOKOGAWA MW100" data acquisition system. The generated power is displayed by a power meter installed in the power controller. All the sensors were carefully calibrated before the experiments. The time-averaged method was applied to reduce the data from the experiments. The time-averaged value is defined as the parameter average value measured for 2 minutes with a sampling rate of 10 Hz under quasi-steady-state condition. Before the start of the experiments, steady state and pressure tests were performed. The variation of average surface temperature was found to be 0.2°C after 15 minutes of operation under steady state condition for heating powers ranging from 10 to 30 W. Therefore in the experiments, a time duration of 15 minutes is considered as the steady state time for recording the data. To evacuate dissolved non-condensable gas in the working fluids, degassing processes were carried out prior to the experiments by heating the working fluids of FC-72 at a heat flux of 4 ~ 5 W/cm^2 for about 45 ~ 50 minutes and opening the valve.

The heating power was increased gradually from 10 W at an interval of 10 W. From the measured temperatures data, the thermocouple uncertainty is ±0.5°C while the pressure

transducer and power meter accuracies are within 0.25% and ±0.3% of their full-scale, respectively. Radial heat loss from the heater was neglected due to the thick insulated heating base which contains two layers of ceramic and Teflon. Only the heat loss in the axial direction was estimated due to the relatively thin insulation layer at the bottom.

Bubble Departure Diameter Measurement. The bubble departure diameter from the graphite foam structure was measured from the captured boiling images using a high speed camera and "Image Pro Software". The isolated bubbles from three different locations (*i.e.* nucleation site) at the graphite foam were used to calculate the bubble diameter. For each location, there are ten (10) bubbles of different captured frames were measured and analyzed by using the software. Hence, the number of measurements are $N = 30$ for each graphite foam evaporator. The measurement method is illustrated in Figure 3.

The average bubble departure diameter ($\overline{D_B}$) and the standard deviation (σ_{D_B}) are calculated by

$$\overline{D_B} = \frac{1}{N}\sum_{i=1}^{N} D_{B_i} \tag{6}$$

$$\sigma_{D_B} = \sqrt{\frac{\sum\left(D_{B_i} - \overline{D_B}\right)^2}{N-1}} \tag{7}$$

Measurement of Bubble Departure Frequency. To determine the bubble departure frequency, the bubble growth and departure processes were recorded by using a high speed camera at 2005 frames per second (fps). The captured images were analyzed frame by frame to determine the bubble growth and departure phenomena. The bubble departure frequency calculation method is portrayed in Figure 4 which shows that a period of bubble growth and departure can be divided into waiting and bubble departure times. Once these times are determined, the bubble departure frequency can be calculated by

$$f_d = \frac{1}{t_w + t_d} \tag{8}$$

Where t_w and t_d are waiting and departure times, respectively. At the frame rate of 2005 fps, the number of frames in the waiting and departure periods are M and N, respectively. Therefore, t_w and t_d can be calculated as

t_w = (M frames/2005 fps) (9)

t_d = (N frames/2005 fps) (10)

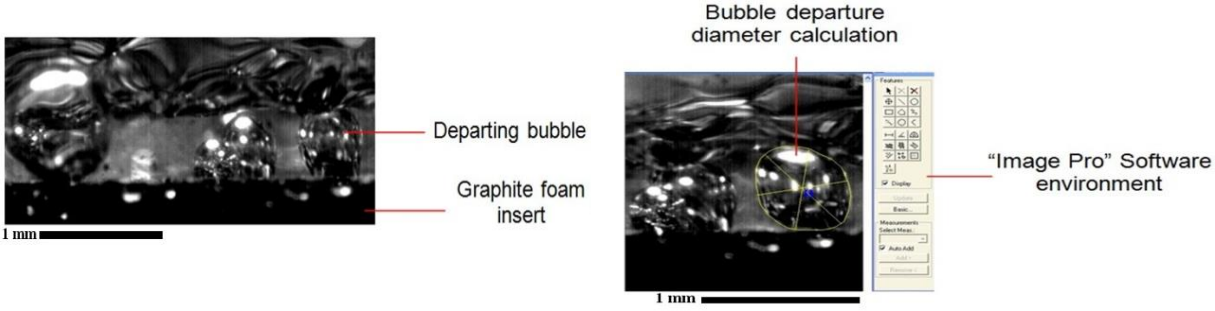

(a) (b)

Figure 3. (a) Typical Captured Images of Boiling on the Graphite Foam Structures and (b) Bubble Departure Diameter Calculation using "Image Pro" Software.

RESULTS AND DISCUSSIONS

Bubble Departure Diameter. From the captured boiling process, bubble growth and departure diameters from different graphite foams and dielectric coolants at heat flux of q'' = 56.34 W/cm^2 are presented in Figure 5(a). It is noted that at q'' = 56.34 W/cm^2, the isolated bubbles from all the graphite foams and working fluids can be observed clearly by using the high speed camera. The average bubble departure diameters and their standard deviations are shown in Table 3. The measurement results show that "Pocofoam" of 61% had produced the smallest bubble departure diameter and bubble growth time compared to other tested graphite foams. The results also show that the measured bubble diameters are much larger as compared to the respective graphite foam pore diameters shown in Table 1. This finding can be used to analyse the boiling heat transfer performance between different graphite foams and the enhancement mechanism from the porous graphite foam structures. The results will also useful to optimise the size in the two-phase cooling system.

Frequency of Bubble Departure. By using the method described in the previous section, the bubble departure frequency from different graphite foams were determined. The results of the bubble departure frequency from the different graphite foams and working fluids are shown in Figure 5(b). It shows that at a heat flux q'' = 56.34 W/cm^2, the measured f_d from the "Pocofoam" 61%, "Pocofoam" 75%, "Kfoam" 78%, and "Kfoam" 72% are 173, 156, 163, and 149 Hz, respectively. It can be found that, "Pocofoam" of 61% produced the highest bubble departure diameter as compared to the other tested graphite foams. The bubble departure frequency values were found to be increased with the increase of heat flux level.

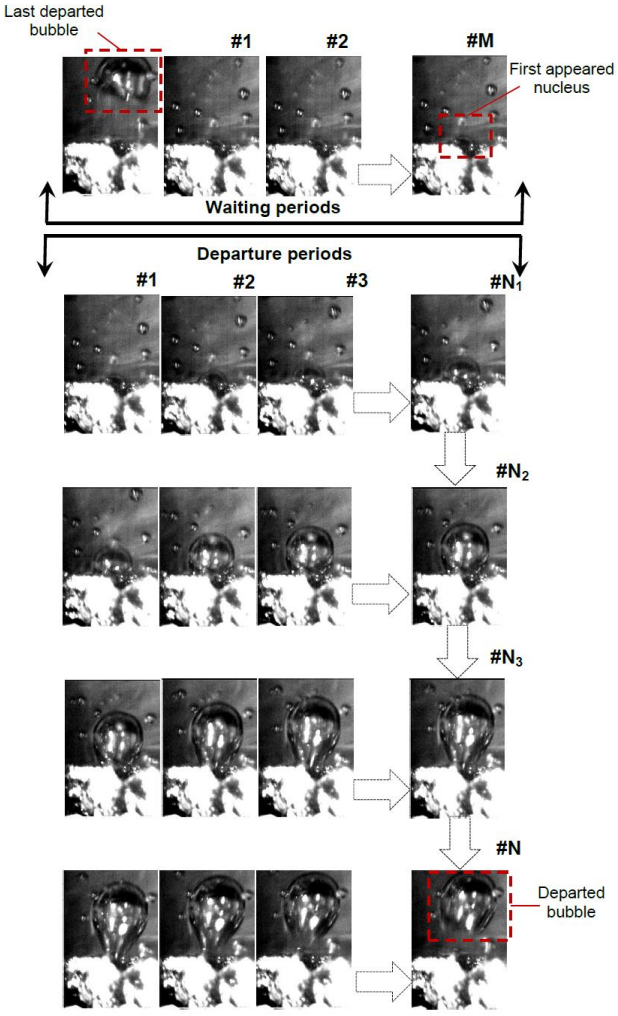

Figure 4. Bubble Departure Frequency Determination.

It is shown that "Kfoam" of 78% porosity have generated higher bubble departure frequency compared to "Pocofoam" of 75% porosity. It is noted from the thermophysical properties of the graphite foams shown in Table 1, "Pocofoam" of 75% porosity possesses higher effective thermal conductivity which is about 2.5 times that of "Kfoam" of 78% porosity. Hence, "Pocofoam" 75% should be more efficient in conducting heat from the heater section to the fluid-solid contact surface where bubble nucleation occurred. Hence, higher bubble frequency should be generated from the "Pocofoam" of 75% porosity. However, the experimental results show that the use of "Kfoam" of 78% porosity resulted in higher bubble departure frequency and boiling performance compared to "Pocofoam" of 75% porosity.

With similar pore structure, the main morphological difference between "Pocofoam" 75% and "Kfoam" 78% is the pore diameter d_P. The pore diameter would affect the bubble departure mechanism and boiling heat transfer significantly.

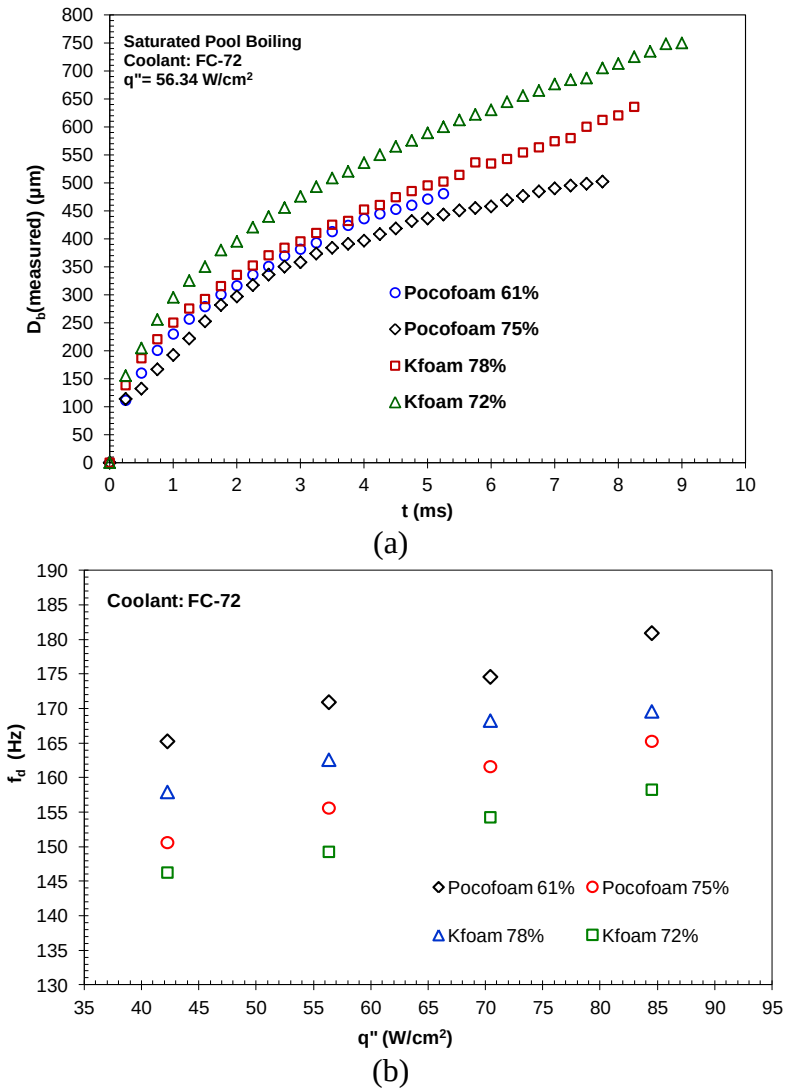

Figure 5. Measured (a) Bubble Departure Diameter and (b) Frequency from the Porous Graphite Foams.

The effect of d_P and other graphite foam parameters to the bubble departure diameter and frequency need to be further explored in the author's future works.

Table 3. The Average and Standard Deviation of D_B at q" = 56.34 W/cm^2

Graphite foam	$\overline{D_B}$ (μm)	σ_{D_B} (μm)
"Pocofoam" 61%	480.8	9.5
"Pocofoam" 75%	502.4	10.2
"Kfoam" 78%	635.8	6.5
"Kfoam" 72%	750.1	8.3

CONCLUSIONS

In this study, the bubble departure diameter and frequency from porous graphite foam structures with FC-72 were studied under saturated pool boiling condition. From this study, the following important findings can be concluded:

1) The thermophysical properties of the graphite foams have affected significantly the bubble departure diameter and frequency. It was also found that the bubble departure frequency values increased linearly with the increase of heat flux level.
2) "Pocofoam" of 61% porosity have produced the smallest bubble departure diameter and highest bubble departure frequency compared to the other graphite foams.
3) The measured bubble departure diameter of the graphite foams were found to be 480.8 ~ 750.1 μm.
4) Bubble departure frequencies of up to 149 ~ 173 Hz were produced by the porous graphite foam structures with FC-72 coolant.

ACKNOWLEDGEMENT

The authors acknowledge the financial supports of the research funding from Department of Mechanical and Industrial Engineering, Faculty of Engineering, Universitas Gadjah Mada 2017 and 2018.

REFERENCES

Chien, L-H. and Webb, R.L., "Measurement of bubble dynamics on an enhanced boiling surfaces," *Experimental Thermal and Fluid Science*, 16, pp. 177-186, (1998).

Cole, R. and Rohsenow, W.M., "Correlation of bubble departure diameters for boiling of saturated liquids," *Chemical Engineering Progress Symposium Series*, 65(92), pp. 211-21, (1968).

Dhir, V.K., Abarajith, H.S., and Li, D., "Bubble dynamics and heat transfer during pool and flow boiling," *Heat Transfer Engineering*, 28(7), pp. 608-624, (2007).

Forster, H.K. and Zuber, N., "Dynamics of vapor bubbles and boiling heat transfer," *AIChE Journal*, 1(4), pp. 531-535, (1955).

Furberg, R., *Enhanced Boiling Heat Transfer on A Dendritic and Micro-Porous Copper Structure*, Ph.D. Thesis, KTH Industrial Engineering and Management, (2011).

Haider, I., *A Theoretical and Experimental Study of Nucleate Pool Boiling Enhancement of Structured Surfaces*, Ph.D. Thesis, Penn State University, (1994).

Han, C-H. and Griffith, P., "The mechanism of heat transfer in nucleate pool boiling-Part I," *International Journal of Heat Mass and Transfer*, 8, pp. 887-904, (1965).

International Technology Road Map for Semiconductor Report 2007, Available at: *http://www.itrs.net/Links/2007ITRS/Home2007.htm* [accessed Sep 5, 2017](2017).

Jin, L.W., Leong, K.C. and Pranoto, I., "Saturated pool boiling heat transfer from highly conductive graphite foams," *Applied Thermal Engineering*, 31, pp. 2685-2693, (2011).

Klett, J.W. and Trammel, M., "Parametric investigation of a graphite foam evaporator in a thermosyphon with fluorinet and silicon CMOS Chip," *IEEE Journal on Device and Materials Reliability*, 4(3), pp. 626-637, (2004).

Koppers Foam Material Data Specification, (2011).

Mudawar, I., "Assessment of high heat flux thermal management schemes," *IEEE Transactions on Component and Packaging Technologies*, 24(2), pp. 122-141, (2001).

Nakayama, W., Daikoku, T., Kuwahara, H., and Nakajima, T., "Dynamic model of enhanced boiling heat transfer on porous surfaces Part II: analytical modelling," *Journal of Heat Transfer*, 102, pp. 451-456, (1980).

Poco Graphite Material Data Specification, (2011).

Pranoto, I., Leong, K.C., and Jin, L.W., "The role of graphite foam pore structure on saturated pool boiling enhancement," *Applied Thermal Engineering*, 42, pp. 163-172, (2012).

White, S.B., Gallego, N.C., Johnson, D.D., Pipe, K., Shih, A.J., and Jih, E., "Graphite foam for cooling of automotive power electronics," *Proceedings of IEEE Power Electronics in Transportation Conference*, USA, pp. 61-65, (2004)

Williams, Z.A. and Roux, J.A., "Graphite foam thermal management of a high packing density array of power amplifiers," *ASME Journal of Electronic Packaging*, 128, pp. 456-465, (2006).

3M Fluorinert Electronic Liquid FC-72 Product Information, (2009).